

Disentangling membrane wetting, compaction, and fouling during ultra-low-pressure liquid filtration using a phase-inverted PVDF membrane

Muhammad Roil Bilad ^{*,1,2}

Afrillia Fahrina ²

Kae Yie Swee ¹

Muthia Elma ³

Yusuf Wibisono ⁴

Sri Mulyati ⁵

Norazanita Shamsuddin ^{*,1}

¹ Faculty of Integrated Technologies, Universiti Brunei Darussalam, Jalan Tungku Link, Bandar Seri Begawan BE1410, Brunei Darussalam

² Cendekia Berkarya Mandiri Foundation, Praya, 83516, Indonesia

³ Chemical Engineering Department, Faculty of Engineering Lambung Mangkurat University, Banjarbaru, South Kalimantan, 70714, Indonesia

⁴ Bioprocess Engineering, University of Brawijaya, Jl. Veteran, Ketawanggede, Kec. Lowokwaru, Kota Malang, Jawa Timur 65145, Indonesia

⁵ Department of Chemical Engineering, Universitas Syiah Kuala, Banda Aceh, Indonesia

*e-mail: roilbilad130@gmail.com (M.R.B); norazanita.shamsudin@ubd.edu.bn (N.S.)

Submitted 17 April 2025

Revised 12 March 2026

Accepted 19 March 2026

Abstract. This study disentangles membrane wetting, compaction, and fouling during ultra-low-pressure filtration using phase-inverted polyvinylidene fluoride (PVDF) membranes. Pressure-stepping tests (0.04-0.11 bar) and repeated one-hour filtration cycles at 0.07 bar, each followed by 10 min of relaxation, were performed with clean water and river water to separate the hydraulic contributions of the three phenomena. With clean water, permeability increased most strongly in the 4-7 kPa range and then approached a plateau, indicating progressive pore wetting. During repeated clean-water filtration, permeability declined because of compaction but recovered from 337.72 to 372.10 L m⁻² h⁻¹ bar⁻¹ after the first relaxation, confirming that part of the compaction was reversible. River water showed consistently lower permeability and only partial recovery (217.40 to 299.30 L m⁻² h⁻¹ bar⁻¹ after the first relaxation), demonstrating the superimposed effect of fouling. The results show that wetting dominates the initial pressure response, compaction governs time-dependent permeability loss under clean water, and fouling becomes decisive in natural water filtration. This mechanistic separation provides a practical basis for pressure optimization, relaxation scheduling, and fouling control in ultra-low-pressure membrane processes.

Keywords: Membrane Compaction, Membrane Fouling, Membrane Wetting, PVDF Membrane, Ultra-Low-Pressure Filtration

INTRODUCTION

Low-pressure membrane processes such as microfiltration and ultrafiltration are widely used in water treatment because they combine compact footprint, good effluent quality, and efficient particle and pathogen removal (Cogan *et al.*, 2016; Sadr & Saroj, 2015). Their wider deployment, however, remains constrained by permeability decline, membrane replacement cost, and the operational burden associated with fouling control (Mecha *et al.*, 2023; Hube *et al.*, 2020).

In practice, permeability loss during low-pressure filtration rarely arises from a single mechanism. Fouling by natural organic matter (NOM), colloids, and other feed constituents adds hydraulic resistance at the membrane surface and inside the pores (Lee *et al.*, 2008; Tian *et al.*, 2018; Yang *et al.*, 2021). At the same time, sustained transmembrane pressure can compact polymeric membranes, reducing pore size and porosity, while incomplete pore wetting can reduce the initial effective transport area (Kallioinen *et al.*, 2007; Stade *et al.*, 2013; Xu *et al.*, 2012). Because these phenomena occur simultaneously, their individual contributions are often confounded, especially under ultra-low-pressure operation, where wetting and compaction can be subtle yet still influential. The magnitude of these effects is further conditioned by membrane morphology and pore characteristics (Filloux *et al.*, 2014; Hung *et al.*, 2022).

PVDF membranes are attractive for such studies because they offer excellent chemical resistance and mechanical stability, but their hydrophobic character can exacerbate wetting limitations and organic fouling (Kim *et al.*, 2015; Fan *et al.*, 2018). Considerable recent work has therefore focused on material-level strategies such as hydrophilic

additives, surface modification, and anti-fouling coatings to improve permeability recovery and fouling resistance (Zhou *et al.*, 2021; Mulyati *et al.*, 2023). These approaches are important, yet operational interpretation remains difficult if wetting, compaction, and fouling are not first distinguished on an unmodified membrane platform.

Earlier studies have independently examined wetting enhancement (Kochan *et al.*, 2009), compaction during ultra-low-pressure filtration (Bilad *et al.*, 2022), hydrodynamic or process-based fouling mitigation strategies (Bu *et al.*, 2019; Rahmawati *et al.*, 2021), and practical ultra-low-pressure applications in complex feeds (Wan Osman *et al.*, 2021; Khery *et al.*, 2022). Nevertheless, a direct experimental framework that separates wetting, compaction, and fouling within a single operating platform remains limited. This limitation also complicates the distinction between reversible resistance and more persistent fouling contributions (Zaouk *et al.*, 2020; Lan *et al.*, 2020).

The present study addresses this gap by evaluating the co-occurrence of wetting, compaction, and fouling during liquid filtration with a phase-inverted PVDF membrane operated at ultra-low pressure. Clean water was used to isolate wetting and compaction, whereas river water introduced natural fouling while preserving the same hydraulic framework. By combining pressure-stepping tests with repeated filtration-relaxation cycles, this work identifies the dominant source of permeability loss under different conditions. It clarifies the practical merit of relaxation in restoring membrane performance.

METHODOLOGY

Materials and Membrane Fabrication

PVDF and N, N-dimethylacetamide (DMAc) were used to prepare the casting solution, while clean water and river water served as feed waters in the filtration experiments. A 15 wt% PVDF solution was prepared by dissolving 3 g of PVDF in 17 g of DMAc under overnight stirring until a homogeneous, bubble-free dope was obtained. The casting solution was then spread onto a nonwoven support placed on a glass plate, with thickness controlled by a casting knife. Phase inversion was initiated by immersing the cast film in a distilled-water coagulation bath, where the membrane solidified. The overall fabrication route is shown in Figure 1.

After solidification, the membrane sheet was removed from the glass plate and prepared for filtration testing. The resulting membrane was handled carefully to preserve its integrity before being mounted in the membrane cell.

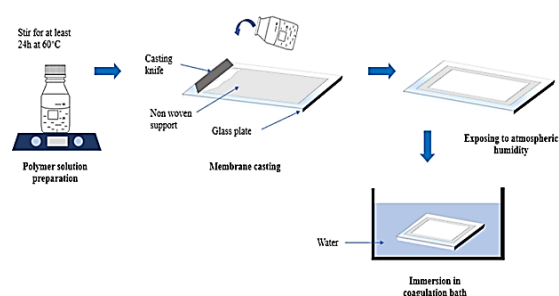


Fig. 1: Illustration of the membrane fabrication process

Filtration Tests

After phase inversion, the membrane sheet was removed from the glass plate, cut into pieces (4.7 cm x 9 cm), and mounted in membrane cells. The cells were sealed to prevent leakage. Feed water was circulated from a feed container using a peristaltic

pump, with the pressure side connected to the membrane cell through a three-way connector and the feed-side pressure monitored by a water manometer. The pump speed was adjusted to set the desired transmembrane pressure. Permeate was collected from the permeate side, whereas the retentate was returned to the feed reservoir.

Two experimental protocols were used. In the pressure-stepping test, the pressure was gradually increased from 0.04 to 0.11 bar, and then decreased, and the experiment was performed twice for both clean water and river water. Between runs, the membrane surface was rinsed with tap water and gently wiped with tissue. In the multiple-filtration test, the membrane was operated at a constant pressure of 0.07 bar for 1 h, followed by 10 min of relaxation; this sequence was repeated four times. Permeate was collected in 150 mL beaker, and the volume was recorded at defined intervals. The resulting flux, J ($L m^{-2} h^{-1}$), and permeability, L_p ($L m^{-2} h^{-1} bar^{-1}$), were calculated from Eqs. (1) and (2), respectively, using the collected permeate volume, filtration time, membrane area, and applied transmembrane pressure.

$$J = \frac{\Delta V}{t A} \quad (1)$$

$$L = \frac{\Delta V}{t A \Delta P} \quad (2)$$

where V is the collected permeate volume, t is filtration time, A is membrane area, and ΔP is the applied transmembrane pressure.

RESULTS AND DISCUSSION

Pressure-Stepping Test

Figures 2 and 3 show the permeability response during pressure stepping with clean

water and river water, respectively. In each case, the pressure was increased stepwise from the low-kPa range to 11 kPa and then decreased, and the experiment was repeated in two runs. This protocol was designed to reveal whether the observed changes in permeability were dominated by progressive wetting, structural compaction, or feed-induced fouling.

For clean water (Figure 2), permeability increased as the pressure rose, especially in the 4-7 kPa range, before tending toward a more stable response at higher pressure. This behavior is characteristic of progressive pore wetting. At the lowest pressures, part of the membrane pore network remains incompletely wetted, so only a fraction of the nominal transport area contributes to permeation. As pressure increases, additional pores become hydraulically active, and the apparent permeability rises (Kochan *et al.*, 2009; Xu *et al.*, 2012). The absence of a clear downward shift with increasing pressure indicates that compaction was not the dominant factor during the relatively short pressure-stepping experiment, which is consistent with the confounding framework discussed by Hung *et al.* (2022).

River-water filtration (Figure 3) followed the same general wetting-driven trend, but the absolute permeability remained lower throughout the test. Because the hydraulic protocol was unchanged, this persistent gap can be attributed to additional resistance from foulants present in the river water, particularly NOM and suspended particulates. Such species are well known to deposit on membrane surfaces and inside pores, thereby increasing filtration resistance even under low-pressure conditions (Lee *et al.*, 2008; Tian *et al.*, 2018; Yang *et al.*, 2021). The slightly better performance of the second run after physical cleaning suggests that part

of the resistance was removable, but the incomplete recovery indicates that some residual fouling remained.

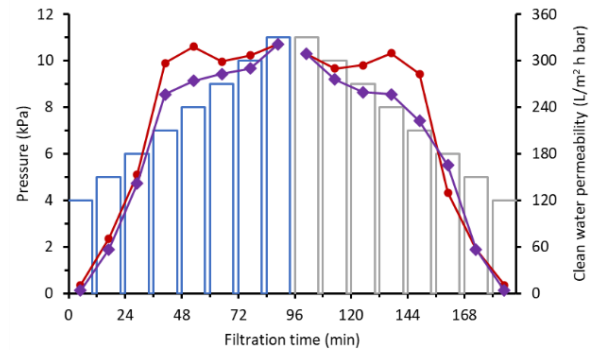


Fig. 2: Clean water permeability from bottom to top and top to bottom showing the two filtration runs

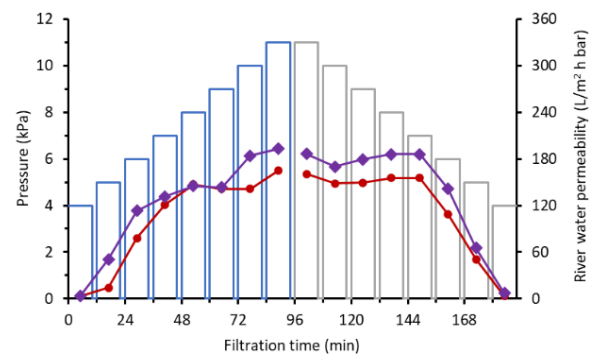


Fig. 3: River water permeability from bottom to top and top to bottom showing the two filtration runs

Taken together, the pressure-stepping experiments show that wetting controls the early pressure response of this PVDF membrane, whereas fouling primarily reduces permeability when natural water is used. This distinction is important because an increase in pressure does not necessarily reflect an intrinsic improvement in membrane structure; rather, it may simply activate previously unwetted pores. This interpretation is also consistent with the broader understanding that membrane material and pore structure condition how feed composition translates into hydraulic

resistance (Filloux *et al.*, 2014; Hube *et al.*, 2020).

Multiple Filtration Test

Figures 4 and 5 present the evolution of permeability during repeated filtration-relaxation cycles at 0.07 bar. Unlike the pressure-stepping test, this protocol emphasizes time-dependent loss of permeability within each one-hour filtration period and the extent to which a 10 min relaxation step can restore performance.

With clean water (Figure 4), the initial permeability was the highest, followed by a progressive decline during each filtration cycle. Because no external foulants were introduced, the dominant source of resistance in this case is membrane compaction. Under sustained transmembrane pressure, polymeric membranes can undergo reversible structural deformation, leading to a temporary reduction in pore size, porosity, or pore connectivity (Kallioinen *et al.*, 2007; Stade *et al.*, 2013). The partial recovery observed after relaxation supports this interpretation. Notably, permeability increased from 337.72 to 372.10 L m⁻² h⁻¹ bar⁻¹ after the first relaxation, showing that part of the permeability loss was recoverable once the compressive stress was removed. This trend agrees with previous reports on ultra-low-pressure membrane compaction in polymeric systems (Bilad *et al.*, 2022; Wan Osman *et al.*, 2021).

River water (Figure 5) showed the same general decline-and-recovery pattern, but at substantially lower permeability. In this case, the observed resistance reflects the combined contribution of compaction and fouling. The presence of NOM and other particulate or colloidal components creates an additional surface and pore-blocking

resistance that relaxation alone cannot fully remove (Sadr & Saroj, 2015; Hube *et al.*, 2020). After the first relaxation, permeability recovered from 217.40 to 299.30 L m⁻² h⁻¹ bar⁻¹, which is appreciable but still clearly below the clean-water level. The result indicates that relaxation can alleviate part of the compaction-related loss, but fouling remains as a more persistent resistance component.

The difference between clean- and river-water behavior also helps distinguish reversible from more persistent resistance. Reversible hydraulic loss is evident from the partial recovery after relaxation. In contrast, the sustained separation between the clean- and river-water profiles indicates foulant deposition that is not removed by a short pressure release alone. This behavior is consistent with the distinction between weakly attached, reversible deposits and more strongly retained material within pores or at the membrane surface (Zaouk *et al.*, 2020; Lan *et al.*, 2020).

These observations have direct operational implications. In relatively clean feeds, pressure management and intermittent relaxation may be sufficient to control reversible compaction and maintain permeability. In more challenging waters, however, hydraulic optimization should be combined with upstream pretreatment, backwashing, or physical-cleaning strategies, or anti-fouling measures such as coagulation, adsorption, spacer-assisted hydrodynamic control, or membrane surface modification (Cogan *et al.*, 2016; Bu *et al.*, 2019; Rahmawati *et al.*, 2021; Zhou *et al.*, 2021). Similar considerations are increasingly important in emerging ultra-low-pressure applications, including biomass harvesting and water recovery from complex wastewater matrices (Khery *et al.*, 2022).

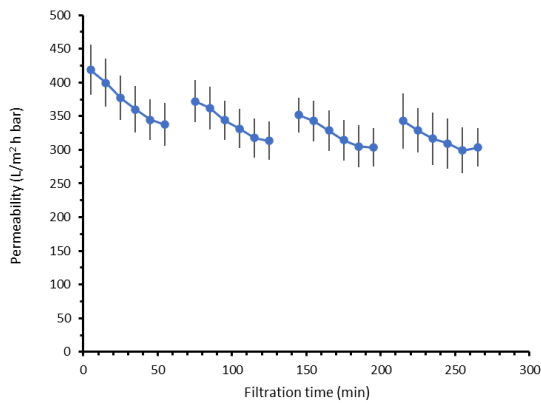


Fig. 4: Permeability evolution of clean water during extended filtration involving relaxation

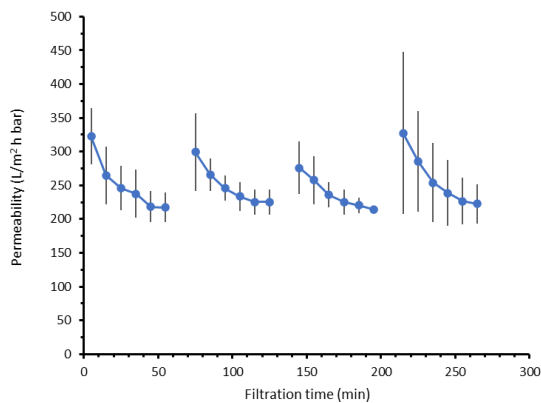


Fig. 5: Permeability evolution of river water during extended filtration involving relaxation

The mechanistic conclusions in the present work are supported by the controlled hydraulic response obtained with clean water and river water, so additional SEM images are not required to justify the main claims. Nevertheless, SEM would be valuable in future studies aimed specifically at visualizing foulant deposition patterns and membrane-fouling mechanisms.

Comparison with Representative Literature

To position the present contribution within the membrane literature, Table 1 summarizes representative studies that

separately emphasize wetting, compaction, anti-fouling material design, or the general confounding of these effects. The comparison shows that the principal merit of the present work is not the introduction of a new membrane material, but the experimental separation of wetting, compaction, and fouling within a single ultra-low-pressure framework using both clean and natural water.

Overall, the table clarifies that the present study complements material-development and application-oriented literature by providing a mechanistic interpretation that can guide both membrane design and operation.

CONCLUSIONS

This work separated the roles of wetting, compaction, and fouling in ultra-low-pressure PVDF membrane filtration using complementary pressure-stepping and repeated filtration-relaxation tests. During pressure stepping, clean-water permeability increased most strongly in the 4–7 kPa range, indicating progressive pore wetting. In contrast, river water showed the same trend at lower absolute permeability due to increased fouling resistance. During repeated filtration at 0.07 bar, clean-water permeability decline was largely attributable to compaction and partially recovered after relaxation, with the first recovery rising from 337.72 to 372.10 L m⁻² h⁻¹ bar⁻¹. River water recovered from 217.40 to 299.30 L m⁻² h⁻¹ bar⁻¹ after the first relaxation, confirming that fouling persisted in addition to compaction. Overall, wetting dominated the initial pressure response, compaction controlled time-dependent losses in clean water, and fouling became decisive in natural water filtration. These findings support a practical

strategy that combines pressure optimization, scheduled relaxation, and targeted fouling control to improve membrane efficiency and durability. Future work may complement this hydraulic analysis with morphological tools such as SEM to further resolve fouling mechanisms and deposit structure.

DECLARATION OF GENERATIVE AI IN SCIENTIFIC WRITING

During the preparation of this work, the authors used ChatGPT to enhance the clarity of the writing. After using ChatGPT, the authors reviewed and edited the content as needed and take full responsibility for the publication's content.

Table 1. Comparison of the present study with representative reports on membrane wetting, compaction, and fouling

Study	System / operating focus	Main contribution	Merit relative to the present study
Kochan et al. (2009)	Polymeric UF membranes; wetting-agent-assisted permeability evaluation	Showed that improved wetting can markedly increase apparent filtration performance by activating previously unwetted pores.	Focuses mainly on wetting and does not separate compaction or natural-water fouling.
Bilad et al. (2022)	Polymeric membrane under ultra-low-pressure water filtration	Established that compaction alone can reduce permeability and that part of the loss is reversible after pressure release.	Addresses compaction in isolation; the present work adds natural-water fouling and pressure-stepping wetting analysis.
Hung et al. (2022)	Review of ultra-low-pressure membrane filtration	Highlighted the confounding effects of wetting, compaction, and fouling and identified the need for clearer experimental separation.	Provides the conceptual basis that the present study validates experimentally.
Wan Osman et al. (2021)	Ultra-low-pressure filtration for microalgae processing	Demonstrated the practical feasibility and energy efficiency of ultra-low-pressure operation in a complex suspension.	Shows application value, whereas the present work isolates the governing hydraulic mechanisms.
Mulyati et al. (2023)	Modified PES membrane for anti-fouling improvement	Improved membrane hydrophilicity and fouling resistance through chitosan-assisted material design.	Represents a material-development strategy; the present work contributes operational and mechanistic interpretation without membrane modification.
Present study	Phase-inverted PVDF membrane; clean water and river water under 0.04-0.11 bar stepping and 0.07 bar repeated filtration	Experimentally disentangles wetting, compaction, and fouling using a common hydraulic platform and relaxation analysis.	Clarifies the dominant source of permeability loss and offers practical guidance for operation under ultra-low-pressure conditions.

REFERENCES

- Bilad, M. R., Junaeda, S. R., Khery, Y., Nufida, B. A., Shamsuddin, N., Usman, A., & Violet, V., 2022. "Compaction of a polymeric membrane in ultra-low-pressure water filtration." *Polymers*, 14(16), 3254. <https://doi.org/10.3390/polym14163254>
- Bu, F., Gao, B., Yue, Q., Liu, C., Wang, W., & Shen, X., 2019. "The combination of coagulation and adsorption for controlling ultra-filtration membrane fouling in water treatment". *Water*, 11(1), 90. <https://doi.org/10.3390/w11010090>
- Cogan, N. G., Li, J., Badireddy, A. R., & Chellam, S., 2016. "Optimal backwashing in dead-end bacterial microfiltration with irreversible attachment mediated by extracellular polymeric substances production". *J. Memb. Sci.*, 520, 337–344. <https://doi.org/10.1016/j.memsci.2016.08.001>
- Fan, H., Xiao, K., Mu, S., Zhou, Y., Ma, J., Wang, X., & Huang, X., 2018. "Impact of membrane pore morphology on multi-cycle fouling and cleaning of hydrophobic and hydrophilic membranes during MBR operation." *J. Memb. Sci.*, 556, 312–320. <https://doi.org/10.1016/j.memsci.2018.04.014>
- Filloux, E., Teychene, B., Tazi-Pain, A., & Croue, J. P., 2014. "Ultrafiltration of biologically treated domestic wastewater: How membrane properties influence performance". *Sep. Pur. Tech.*, 134, 178–186. <https://doi.org/10.1016/j.seppur.2014.07.043>
- Hube, S., Eskafi, M., Hrafnkelsdóttir, K. F., Bjarnadóttir, B., Bjarnadóttir, M. Á., Axelsdóttir, S., & Wu, B., 2020. "Direct membrane filtration for wastewater treatment and resource recovery: A review". *Sci. Total. Env.*, 710, 136375. <https://doi.org/10.1016/j.scitotenv.2019.136375>
- Hung, T. S., Bilad, M. R., Shamsuddin, N., Suhaimi, H., Ismail, N. M., Jaafar, J., & Ismail, A. F., 2022. "Confounding effect of wetting, compaction, and fouling in an ultra-low-pressure membrane filtration: A review." *Polymers*, 14(10), 2073. <https://doi.org/10.3390/polym14102073>
- Kallioinen, M., Pekkarinen, M., Mänttari, M., Nuortila-Jokinen, J., & Nyström, M., 2007. "Comparison of the performance of two different regenerated cellulose ultrafiltration membranes at high filtration pressure". *J. Memb. Sci.*, 294(1–2), 93–102. <https://doi.org/10.1016/j.memsci.2007.02.016>
- Khery, Y., Daniar, S. E., Mat Nawi, N. I., Bilad, M. R., Wibisono, Y., Nufida, B. A., Ahmadi, A., Jaafar, J., Huda, N., & Kobun, R., 2022. "Ultra-low-pressure membrane filtration for simultaneous recovery of detergent and water from laundry wastewater." *Membranes*, 12(6), 591. <https://doi.org/10.3390/membranes12060591>
- Kim, T. H., Jee, K. Y., & Lee, Y. T., 2015. "The improvement of water flux and mechanical strength of PVDF hollow fiber membranes by stretching and annealing conditions." *Macromol. Res.*, 23(7), 592–600. <https://doi.org/10.1007/s13233-015-3087-0>
- Kochan, J., Wintgens, T., Hochstrat, R., & Melin, T., 2009. "Impact of wetting agents on the filtration performance of polymeric ultrafiltration membranes."
-

-
- Desalination*, 241(1–3), 34–42.
<https://doi.org/10.1016/j.desal.2008.01.056>
- Lan, Y., Barthe, L., Azais, A., & Causserand, C., 2020. "Feasibility of a heterogeneous Fenton membrane reactor containing a Fe-ZSM5 catalyst for pharmaceuticals degradation: Membrane fouling control and long-term stability." *Sep. Pur. Tech.*, 231, 115920.
<https://doi.org/10.1016/j.seppur.2019.115920>
- Lee, E. K., Chen, V., & Fane, A. G. 2008. "Natural organic matter (NOM) fouling in low pressure membrane filtration—Effect of membranes and operation modes." *Desalination*, 218(1–3), 257–270.
<https://doi.org/10.1016/j.desal.2007.02.021>
- Mecha, A. C., Chollom, M. N., Babatunde, B. F., Tetteh, E. K., & Rathilal, S., 2023. "Versatile silver-nanoparticle-impregnated membranes for water treatment: A review." *Membranes*, 13(4), 432.
<https://doi.org/10.3390/membranes13040432>
- Mulyati, S., Rosnelly, C. M., Syamsuddin, Y., Arahman, N., Muchtar, S., Wahyuni, W., Lauzia, T., Ambarita, A. C., Bilad, M. R., & Samsuri, S., 2023. "Enhancing the anti-fouling property of polyethersulfone-based membrane using chitosan additive from golden snail (*Pomacea canaliculata*) shell waste for water purification." *ASEAN J. Chem. Eng.*, 23(2), 224–239.
<https://doi.org/10.22146/ajche.79643>
- Rahmawati, R., Bilad, M. R., Nawi, N. I. M., Wibisono, Y., Suhaimi, H., Shamsuddin, N., & Arahman, N., 2021. "Engineered spacers for fouling mitigation in pressure driven membrane processes: Progress and projection." *J. Env. Chem. Eng.*, 9(5), 106285.
<https://doi.org/10.1016/j.jece.2021.106285>
- Sadr, S. M. K., & Saroj, D. P., 2015. "Membrane technologies for municipal wastewater treatment". In *Adv. Memb. Tech. Water. Treat.*, 443–463.
<https://doi.org/10.1016/B978-1-78242-121-4.00014-9>
- Stade, S., Kallioinen, M., Mikkola, A., Tuuva, T., & Mänttari, M., 2013. "Reversible and irreversible compaction of ultrafiltration membranes." *Sep. Pur. Tech.*, 118, 127–134.
<https://doi.org/10.1016/j.seppur.2013.06.039>
- Tian, J., Wu, C., Yu, H., Gao, S., Li, G., Cui, F., & Qu, F., 2018. "Applying ultraviolet/persulfate (UV/PS) pre-oxidation for controlling ultrafiltration membrane fouling by natural organic matter (NOM) in surface water." *Water Res.*, 132, 190–199.
<https://doi.org/10.1016/j.watres.2018.01.005>
- Wan Osman, W. N. A., Mat Nawi, N. I., Samsuri, S., Bilad, M. R., Khan, A. L., Hunaepi, H., Jaafar, J., & Lam, M. K., 2021. "Ultra low-pressure filtration system for energy efficient microalgae filtration." *Heliyon*, 7(6), e07367.
<https://doi.org/10.1016/j.heliyon.2021.e07367>
- Xu, Q., Yang, Y., Wang, X., Wang, Z., Jin, W., Huang, J., & Wang, Y., 2012. "Atomic layer deposition of alumina on porous polytetrafluoroethylene membranes for enhanced hydrophilicity and separation performances." *J. Memb. Sci.*, 415–416, 435–443.
<https://doi.org/10.1016/j.memsci.2012.0>
-

-
- 5.031
- Yang, F., Huang, Z., Huang, J., Wu, C., Zhou, R., & Jin, Y., 2021. "Tanning wastewater treatment by ultrafiltration: Process efficiency and fouling behavior." *Membr.*, *11*(7), 461. <https://doi.org/10.3390/membranes11070461>
- Zaouk, L., Massé, A., Bourseau, P., Taha, S., Rabiller-Baudry, M., Jubeau, S., Teychené, B., Pruvost, J., & Jaouen, P., 2020. "Filterability of exopolysaccharides solutions from the red microalga *Porphyridium cruentum* by tangential filtration on a polymeric membrane." *Env. Tech.*, *41*(9), 1167–1184. <https://doi.org/10.1080/09593330.2018.1523234>
- Zhou, X., Sun, Y., Shen, S., Li, Y., & Bai, R., 2021. "Highly effective anti-organic fouling performance of a modified PVDF membrane using a triple-component copolymer of P(Stx-co-MAAy)-g-fPEGz as the additive". *Membranes*, *11*(12), 951. <https://doi.org/10.3390/membranes11120951>
-